Measurement of absolute frequencies and hyperfine structure constants of $4D_{5/2}$ and $4D_{3/2}$ levels of ^{87}Rb and ^{85}Rb using an optical frequency comb

Won-Kyu Lee[1] and Han Seb Moon[2,*]

[1]*Korea Research Institute of Standards and Science, Daejeon 305-340, Korea*

[2]*Department of Physics, Pusan National University, Busan 609-735, Korea*

(Received 15 April 2015; published 1 July 2015)

We report the absolute frequency values of all (ten) hyperfine transitions of $5P_{3/2} - 4D_{5/2}$ and $5P_{3/2} - 4D_{3/2}$ for ^{87}Rb and ^{85}Rb atoms via the use of an optical frequency comb by measuring the frequency of a laser diode stabilized onto the line centers of the double-resonance optical pumping spectra. Here we report on the absolute frequencies for the two transitions [^{85}Rb, $5P_{3/2}(F' = 4) - 4D_{5/2}(F'' = 3,4)$]. Furthermore, the frequency uncertainties are reduced significantly for the other transitions. Moreover, the magnetic dipole and the electric quadrupole hyperfine structure constants of $4D_{5/2}$ for ^{87}Rb and ^{85}Rb are determined by using the measured values of the absolute frequency.

DOI: 10.1103/PhysRevA.92.012501 PACS number(s): 32.10.Fn, 42.62.Fi, 32.30.−r

I. INTRODUCTION

Atomic electron transition lines have been commonly used to provide absolute frequency references. Although the atomic transition lines between excited states are frequently used in high-resolution spectroscopy, the spectroscopic data for these transition lines is often insufficient. This is due to the inherent experimental disadvantage of the conventional optical-optical double-resonance (OODR) method [1,2]; the intermediate state can hardly be populated sufficiently in a system with a fast-decaying channel to other energy levels. Thus, the signal-to-noise ratio (SNR) of the excited-state transition is very poor, except for the cases of the cycling transitions. In contrast, through detection of the population of the ground state instead of the intermediate state, the recently developed experimental method, called the double-resonance optical pumping (DROP) method [3,4], can overcome this limitation, producing a good SNR, even in the cases of noncycling transitions.

The $5P_{3/2} - 4D_{5/2}$ and $5P_{3/2} - 4D_{3/2}$ transitions of rubidium atoms have attracted attention as optical communication frequency references. Sasada [1] measured the absolute frequencies for six of these transitions for the first time by using a calibrated wavelength meter and OODR spectroscopy. Fifteen years later, by exploiting the DROP method, Lee *et al.* reported the absolute frequency values of the $5P_{3/2} - 4D_{5/2}$ transition for ^{87}Rb [5] and the $5P_{3/2} - 4D_{3/2}$ transitions for ^{87}Rb and ^{85}Rb [6] with a femtosecond frequency comb. The uncertainty determined in their work exhibited a decrease by 3 orders of magnitude when compared with that reported in Ref. [1].

The hyperfine structure (HFS) constants of the $4D$ state of the Rb atom have been measured by means of various experimental methods, including cascaded-radio frequency-spectroscopy [7], the OODR method [2], and the DROP method [5,8]. Lee *et al.* [5] determined the magnetic dipole HFS constant of the $4D_{5/2}$ state for ^{87}Rb by using the DROP method with the uncertainty reduced 60-fold compared with a previous result [7] and the electric quadrupole HFS constant of the $4D_{5/2}$ state for the first time. Recently, Wang *et al.* [8] have reported the magnetic dipole and electric quadrupole HFS constants of the $4D_{5/2}$ state for both ^{87}Rb and ^{85}Rb by measuring the HFS splitting in the DROP spectra, of which frequency was calibrated by means of a scanning Fabry-Pérot cavity and a wideband fiber-pigtailed electro-optic modulator.

In this paper we report the absolute frequency values of all (ten) of the $5P_{3/2} - 4D_{5/2}$ and $5P_{3/2} - 4D_{3/2}$ transitions for ^{87}Rb and ^{85}Rb between the excited HFS energy levels using the DROP method and an optical frequency comb. Here we report on the absolute frequencies for the two transitions [^{85}Rb, $5P_{3/2}(F' = 4) - 4D_{5/2}(F'' = 3,4)$]. Furthermore, the frequency uncertainty for one transition reduced by 3 orders of magnitude compared with the previous measurement by a wavelength meter. In addition, this report provides modified values for three absolute frequencies of the $5P_{3/2} - 4D_{5/2}$ transition of ^{87}Rb by using a linear-parallel polarization configuration in contrast to the linear-orthogonal polarization used in Ref. [5]. As the complete set of the absolute frequency values were obtained under the same experimental conditions for all the possible transitions, our results can be useful for comparison purposes with other reported values that cover only a part of all the transitions. Finally, the HFS constants of $4D_{5/2}$ for ^{87}Rb and ^{85}Rb were obtained using the absolute frequency measurement data, and these were compared with previous reports. We believe that our results can also aid in testing theoretical calculations [9,10] and HFS anomalies [8], because there are difficulties in the computation with the D states due to strong correlation effects.

II. EXPERIMENT

Figure 1 shows the HFS of ^{87}Rb and ^{85}Rb, which are two naturally occurring isotopes with abundances of 27.8% and 72.2%, respectively, for the $5S_{1/2} - 5P_{3/2} - 4D_{5/2}$ transitions in Fig. 1(a) and for the $5S_{1/2} - 5P_{3/2} - 4D_{3/2}$ transitions in Fig. 1(b). When the first laser diode (LD1 in the DROP setup) is resonant with the cycling transition of the Rb D_2 line [$5S_{1/2}(F = 2) - 5P_{3/2}(F' = 3)$ of ^{87}Rb and $5S_{1/2}(F = 3) - 5P_{3/2}(F' = 4)$ of ^{85}Rb], the numbers of the HFS components that satisfy the selection rule for the second laser diode (LD2) are three for the $4D_{5/2}$ state and two for the $4D_{3/2}$ state, as shown in Fig. 1. The HFS components interacting with LD1 and LD2 are represented by black lines and the other noninteracting HFS components by gray lines in Fig. 1.

*Corresponding author: hsmoon@pusan.ac.kr

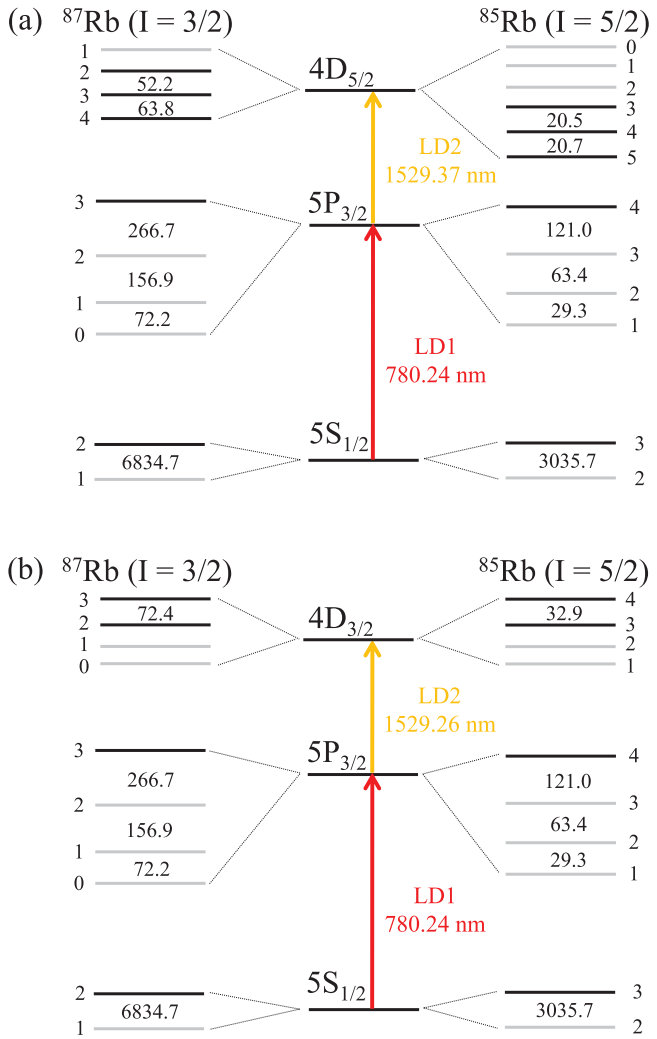

FIG. 1. (Color online) Hyperfine structures of ^{87}Rb and ^{85}Rb for the (a) $5S_{1/2} - 5P_{3/2} - 4D_{5/2}$ transitions and (b) for the $5S_{1/2} - 5P_{3/2} - 4D_{3/2}$ transitions. The numbers between the energy levels represent the numerical values of the hyperfine splitting in megahertz. The values of the total angular momentum (F) are indicated by the small numerals immediately adjacent to each energy level.

The experimental setup for DROP spectroscopy, laser frequency stabilization, and absolute frequency measurement is shown in Fig. 2. This setup is similar to those described in previous reports [5,6], except for the use of a three-dimensional Helmholtz coil (for better controllability of the magnetic field) replacing the μ-metal shields in the previous setup. Two grating-feedback external-cavity laser diodes were used for the DROP experiment. The frequency of the probe laser (LD1 at 780 nm) was stabilized to the cycling transition in the Rb D_2 line ($5S_{1/2} - 5P_{3/2}$) using a conventional technique for saturated absorption spectroscopy (SAS) in a 5-cm-long Rb vapor cell. The frequency of LD1 was modulated by a piezoelectric transducer (PZT) in the external cavity for SAS with a modulation depth of about 5 MHz and modulation frequency of 5 kHz. The frequency of the pump laser (LD2 at 1529 nm) was tuned to be resonant with the $5P_{3/2} - 4D_{5/2}$ or $5P_{3/2} - 4D_{3/2}$ transitions. The lasers LD1 and LD2 were counterpropagating in a 10-cm-long Rb vapor cell at room

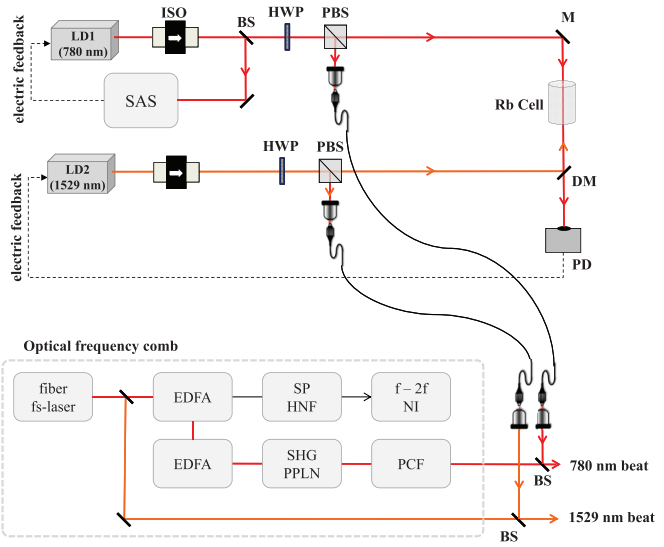

FIG. 2. (Color online) Experimental setup for double-resonance optical pumping (DROP) spectroscopy and absolute frequency measurement. ISO, optical isolator; BS, beam splitter; SAS, saturated absorption spectroscopy setup; HWP, half-wave plate; PBS, polarizing beam splitter; M, mirror; DM, dichroic mirror; PD, Si photodiode; EDFA, erbium-doped fiber amplifier; SFG-PPLN, periodically polled lithium niobate for the second-harmonic generation; SP-HNF, highly nonlinear fiber for spectral broadening; f-2f NI, f-to-2f nonlinear interferometer; PCF, photonic crystal fiber.

temperature. The two laser beams were made to overlap within 1 mrad with the use of two apertures with a diameter of 1.5 mm. The polarizations of both lasers were linear and parallel to each other in the 10-cm-long Rb vapor cell at room temperature. The magnetic field was cancelled by using a three-dimensional Helmholtz coil. The residual magnetic field was less than 1 μT. The optical powers of LD1 and LD2 entering the Rb cell, which were controlled by polarizing-beam-splitter and half-wave-plate pairs, were measured to be 15 and 30 μW, respectively. In order to obtain the DROP spectrum, the frequency of LD2 was scanned over the range of the upper states ($4D_{5/2}$ or $4D_{3/2}$) and LD1 was probed. We measured the transmission of LD1 with a dichroic mirror (DM; reflection at 1529 nm, transmission at 780 nm) and a Si photodiode to obtain the DROP spectrum.

The typical DROP spectra are shown in Fig. 3. The spectral widths were approximately 6 MHz, which agrees with the estimated results under the two-photon resonance condition [4]. The frequency of LD2 was stabilized on one of the peaks (i.e., one of the hyperfine components) of the DROP signal. Additional frequency modulation of LD2 was not necessary because LD1 was already modulated for stabilization using SAS. The first-harmonic error signal of the DROP spectrum was fed back to the PZT of LD2 for frequency stabilization.

The absolute frequencies of the stabilized lasers were measured by means of an optical frequency comb capable of covering two octaves. The comb was based on a fiber femtosecond laser centered at 1550 nm. The repetition rate (250 MHz) was phase locked using a frequency synthesizer, which was referenced to a hydrogen maser that was calibrated

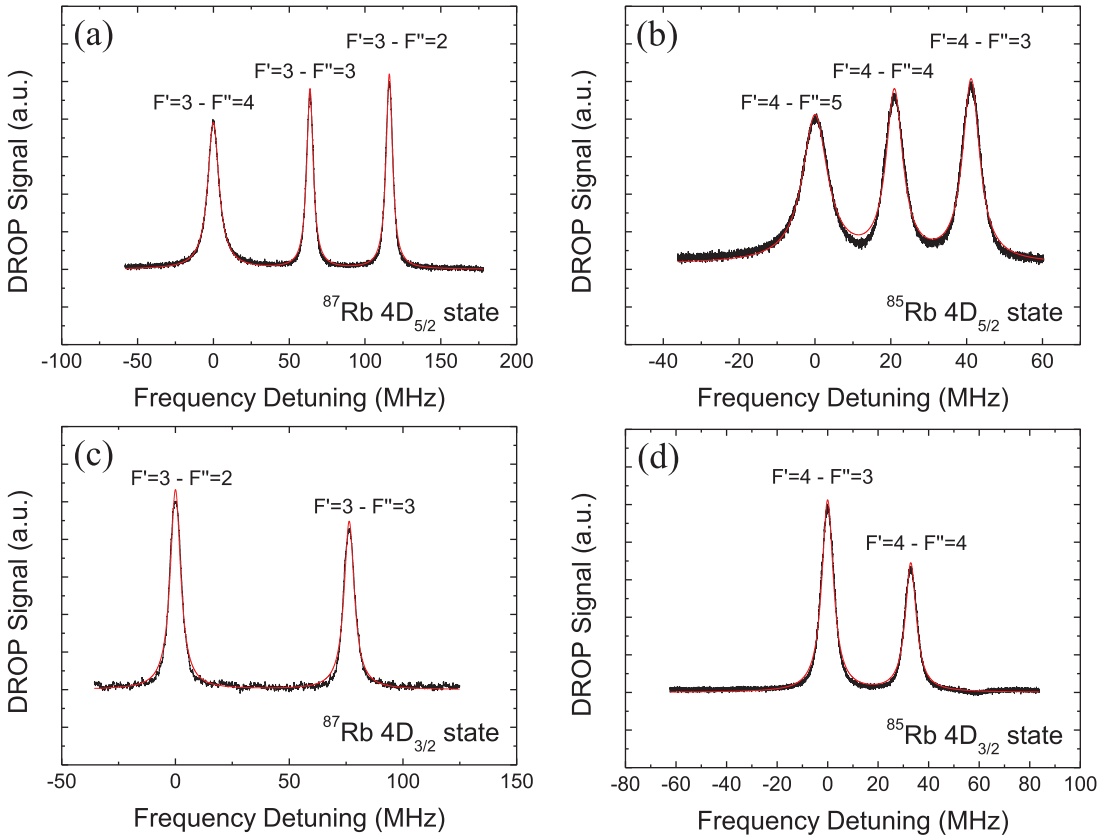

FIG. 3. (Color online) Typical double-resonance optical pumping (DROP) spectra (black lines) and multi-Lorentzian-fitted curves (red lines) of (a) $5P_{3/2}(F'=3)-4D_{5/2}(F''=2,3,4)$ transitions of ^{87}Rb, (b) $5P_{3/2}(F'=4)-4D_{5/2}(F''=3,4,5)$ transitions of ^{85}Rb, (c) $5P_{3/2}(F'=3)-4D_{3/2}(F''=3,2)$ transitions of ^{87}Rb, and (d) $5P_{3/2}(F'=4)-4D_{3/2}(F''=4,3)$ transitions of ^{85}Rb.

to the SI (the International System of Units) second through the Global Positioning System. This fiber comb has a two-branch configuration [11]. In our study, the signal in one branch was amplified by an erbium-doped fiber amplifier (EDFA) and was spectrally broadened to the wavelength range from 1050 to 2100 nm using a highly nonlinear fiber (HNF) in order to measure the infrared frequency and to stabilize the carrier envelope offset (CEO) frequency by means of the well-known f-to-$2f$ self-referencing technique. The CEO frequency was phase locked to a 20-MHz signal referenced to the same hydrogen maser as that used in the repetition rate stabilization. All the counters used in the experiment were also referenced to this hydrogen maser. The signal in the second branch of the fiber comb was amplified by another EDFA, and the output was frequency doubled by means of a periodically poled lithium niobate (PPNL) crystal. The spectrum of this frequency-doubled comb was broadened further by a photonic crystal fiber (PCF) to cover the wavelength range from 500 to 1000 nm. The absolute frequencies of LD1 and LD2 were simultaneously measured by using this two-octave-spanning optical frequency comb. The two laser outputs were delivered to the frequency comb using 30-m-long single-mode fibers for the respective wavelengths. Each beat-note frequency between one of the two stabilized lasers and the fiber comb was measured using a correspondingly separate avalanche photodetector and frequency counter. We were also able to measure the frequency stabilities of the pump and the probe lasers via the optical frequency-comb measurement. The frequency stability of LD1 in terms of the Allan deviation was 5.0×10^{-12} for an averaging time of 1 s and 7×10^{-13} for 128 s. The frequency stability of LD2 was 1.0×10^{-11} at 1 s, and it decreased to 1.3×10^{-12} at 128 s [6].

III. ABSOLUTE FREQUENCY MEASUREMENTS

The frequency of the probe laser, which was locked onto the $5S_{1/2}-5P_{3/2}$ transition at 780 nm, was measured via the frequency-doubled fiber comb spectrum. The SNR of the heterodyne beat signal between LD1 and the fiber comb was greater than 30 dB in a resolution bandwidth (RBW) of 400 kHz, which is sufficient for the correct frequency counting. The absolute frequency of the $5S_{1/2}(F=2)-5P_{3/2}(F'=3)$ transition of ^{87}Rb was measured to be 384 228 115 208(17) kHz and that of the $5S_{1/2}(F=3)-5P_{3/2}(F'=4)$ transition of ^{85}Rb to be 384 229 241 999(17) kHz, which agree well with previous reports [12–14]. The frequency uncertainty was estimated by means of the long-term frequency drift of LD1 over 2 months.

Simultaneously, the absolute frequenciee $5P_{3/2}-4D_{5/2}$(or $4D_{3/2}$) transitions at 1529 nm, were measured by the fiber comb infrared output. We ensured that the SNR of the beat signal between LD2 and the fiber comb was greater than 30 dB in an RBW of 400 kHz. We measured the absolute frequency under our standard conditions; i.e., the optical

TABLE I. Measurement results of the absolute frequencies of the $5P_{3/2} - 4D_{5/2}$ and $5P_{3/2} - 4D_{3/2}$ transitions for ^{87}Rb and ^{85}Rb.

Transition	Absolute frequency (MHz)
^{87}Rb, $5P_{3/2}(F' = 3) - 4D_{5/2}(F'' = 2)$	196023851.304 ± 0.016
^{87}Rb, $5P_{3/2}(F' = 3) - 4D_{5/2}(F'' = 3)$	196023799.116 ± 0.024
^{87}Rb, $5P_{3/2}(F' = 3) - 4D_{5/2}(F'' = 4)$	196023735.290 ± 0.042
^{85}Rb, $5P_{3/2}(F' = 4) - 4D_{5/2}(F'' = 3)$	196023817.926 ± 0.018
^{85}Rb, $5P_{3/2}(F' = 4) - 4D_{5/2}(F'' = 4)$	196023797.464 ± 0.039
^{85}Rb, $5P_{3/2}(F' = 4) - 4D_{5/2}(F'' = 5)$	196023776.715 ± 0.047
^{87}Rb, $5P_{3/2}(F' = 3) - 4D_{3/2}(F'' = 3)$	196037213.796 ± 0.020
^{87}Rb, $5P_{3/2}(F' = 3) - 4D_{3/2}(F'' = 2)$	196037137.412 ± 0.022
^{85}Rb, $5P_{3/2}(F' = 4) - 4D_{3/2}(F'' = 4)$	196037194.590 ± 0.018
^{85}Rb, $5P_{3/2}(F' = 4) - 4D_{3/2}(F'' = 3)$	196037161.679 ± 0.023

powers entering the Rb cell were 15 and 30 μW for LD1 and LD2, respectively, the polarizations of both lasers were linear and parallel to each other, and the probe laser modulation depth was 5 MHz. The absolute frequency measurement results of the $5P_{3/2} - 4D_{5/2}$ and $5P_{3/2} - 4D_{3/2}$ transitions for ^{87}Rb and ^{85}Rb are summarized in Table I.

This result reports on the absolute frequencies for two of the transitions listed in Table I, [^{85}Rb, $5P_{3/2}(F' = 4) - 4D_{5/2}(F'' = 3,4)$]. Sasada [1] measured the absolute frequencies for six of the transitions listed in Table I with an uncertainty of 40 MHz by using a wavelength meter and OODR spectroscopy [for four transitions of $5P_{3/2} - 4D_{3/2}$ and for two cycling transitions of $5P_{3/2} - 4D_{5/2}$, that is, $5P_{3/2}(F' = 3) - 4D_{5/2}(F'' = 4)$ for ^{87}Rb, and $5P_{3/2}(F' = 4) - 4D_{5/2}(F'' = 5)$ for ^{85}Rb]. The results of our report agree well with this previous investigation, and our results provide far more accurate frequency values for these six transitions with uncertainties reduced by 3 orders of magnitude. Further, for the four transitions of $5P_{3/2} - 4D_{3/2}$, these new measurement results agree well with the previous results obtained by our group [6], and the uncertainties are reduced by more than 4 times, mainly due to better control of the magnetic field and polarization angle. In Ref. [5], a linear-orthogonal polarization was used for LD1 and LD2 for the transitions of $5P_{3/2}(F' = 3) - 4D_{5/2}(F'' = 2,3,4)$ of ^{87}Rb. This report provides the modified values for these three transitions in the case of a linear-parallel polarization configuration.

The uncertainty budgets in determining the absolute frequencies are summarized in Table II. The uncertainty components include the polarization angle, magnetic field, cell dependence, laser powers of both LD1 and LD2, dc offset in the frequency lock, modulation depth of LD1, short-term statistical uncertainty in the fiber comb measurement, long-term repeatability, and uncertainty in the compensation of frequency pulling by adjacent spectral peaks. The effects from the relativistic shift, collision shift, and blackbody radiation are ignored because these are relatively small.

We determined that a major part of the frequency uncertainty was due to the polarization angle of the laser beams in our experiment. The direction of external magnetic field and the polarization vector of the laser may distort the spectral shape of the DROP spectrum, because the atomic

TABLE II. Uncertainty budget in determining the absolute frequencies of $5P_{3/2} - 4D_{5/2}$ and $5P_{3/2} - 4D_{3/2}$ transitions for ^{87}Rb and ^{85}Rb.

		Frequency uncertainty (kHz)									
		Transition									
		^{87}Rb, $5P_{3/2} - 4D_{5/2}$			^{85}Rb, $5P_{3/2} - 4D_{5/2}$			^{87}Rb, $5P_{3/2} - 4D_{3/2}$		^{85}Rb, $5P_{3/2} - 4D_{3/2}$	
Effect	Uncertainty of effect	$F'' = 2$	$F'' = 3$	$F'' = 4$	$F'' = 3$	$F'' = 4$	$F'' = 5$	$F'' = 3$	$F'' = 2$	$F'' = 4$	$F'' = 3$
Polarization angle	20 deg	6.8	18	38	11	36	44	14	17	10	17
B field (B_x)	20 mG	0.14	0.59	0.41	0.57	0.93	1.4	0.48	0.55	0.17	0.74
B field (B_y)	20 mG	1.6	1.8	4.3	1.3	1.8	2.7	1.3	1.3	1.4	0.98
B field (B_z)	20 mG	1.8	2.0	5.8	0.64	2.2	5.7	2.0	2.2	1.3	2.0
Cell dependence		9.5	9.5	9.5	9.5	9.5	9.5	9.5	9.5	9.5	9.5
LD2 power	3 μW (10%)	1.9	4.1	8.7	6.2	7.9	7.1	6.0	6.0	6.0	6.0
LD1 power	1.5 μW (10%)	1.5	1.5	1.5	2.0	2.0	2.0	2.0	2.0	2.0	2.0
Lock dc offset	1 mV	6.6	6.6	6.6	2.1	1.5	1.6	4.2	4.2	4.2	4.2
LD1 mod. depth		1.0	1.0	1.0	1.0	1.0	1.0	1.0	1.0	1.0	1.0
Statistical (fs comb)	Short-term	0.16	0.08	0.12	0.05	0.06	0.06	0.30	0.30	0.30	0.30
Repeatability	Long-term	7.0	7.0	7.0	7.0	7.0	7.0	7.0	7.0	7.0	7.0
Frequency pulling by adjacent peaks	(Shifts indicated in parentheses)	0.01 (−0.33)	0.03 (−0.10)	0.20 (+0.73)	1.8 (−6.53)	1.0 (−3.96)	4.4 (+15.81)	0.04 (−0.14)	0.03 (+0.10)	0.59 (−2.11)	0.26 (+0.95)
Total		16	24	42	18	39	47	20	22	18	23

TABLE III. Hyperfine structure constants of $4D_{5/2}$ for ^{87}Rb and ^{85}Rb (in MHz).

Reference	A^{87}	A^{85}	B^{87}	B^{85}	Method
Liao, 1974 [7]	−16.9(6)	−5.2(3)			Cascade RF spectroscopy
Sinclair, 1994 [2]		−5.06(10)		7.42(15)	Fabry-Pérot interferometer with cold atom OODR
Lee, 2007 [5]*	−16.747(10)		4.149(59)		Femtosecond comb with DROP, *(linear-orthogonal polarization)
Wang, 2014 [8]	−16.801(5)	−4.978(4)	3.645(30)	6.560(52)	Fabry-Pérot cavity with DROP
This work	−16.779(6)	−5.008(9)	4.112(52)	7.15(15)	Femtosecond comb with DROP

transitions between Zeeman sublevels have different routes according to the laser polarization, and the atomic-magnetic momentum changes according to the static magnetic fields. In general, the quantization axis is taken to be in the direction of an external magnetic field. When the propagation direction of the linearly polarized laser and the quantization axis are perpendicular, π ($\Delta m = 0$) transitions can be induced between Zeeman sublevels. If the quantization axis is parallel to the direction of a laser propagation, σ^+ ($\Delta m = +1$) and σ^- ($\Delta m = -1$) transitions can be induced between Zeeman sublevels. However, if there is residual magnetic field, there can be arbitrary atomic transitions. This effect was attributed to the residual Zeeman effect by the uncancelled magnetic field and the possible birefringence of the dichroic mirrors and the vapor cell window. The polarization uncertainty occurs due to the birefringence, and the quantum axis is not certain because we do not know the direction of the uncancelled magnetic field. To evaluate the uncertainty due to the polarization, we varied the mutual polarization angle between LD1 and LD2 using a half-wave plate before LD1 entrance, and we measured the shift in the absolute frequency for each of the ten transitions. The uncertainty of the polarization angle was taken to be 20 deg. The frequency uncertainty due to the magnetic field was investigated by varying the current in each axis of the three-dimensional Helmholtz coil, which was originally used for the magnetic field cancellation. The uncertainty of the magnetic field cancellation was taken to be 2 μT. The typical value of the cell dependence was evaluated by using three different Rb vapor cells and measuring the absolute frequency of the $5P_{3/2}(F' = 3) - 4D_{5/2}(F'' = 4)$ transition for ^{87}Rb. The frequency uncertainty related to the power levels of the lasers was investigated by varying the power of one laser with that of the other fixed at the standard power value (15 μW for LD1 and 30 μW for LD2). We assumed the uncertainty of the laser power as 10% of its standard value. It is to be noted here that the offsets in the lock electronics can also cause frequency shifts. By measuring the change in the absolute frequency of the transitions, we estimated the frequency uncertainty by considering the lock dc offset to be 1 mV. The typical frequency uncertainty caused by LD1 modulation, which was used for the frequency stabilization of the probe laser by the SAS method, was investigated using the $5P_{3/2}(F' = 4) - 4D_{5/2}(F'' = 5)$ transition of ^{85}Rb. The short-term statistical uncertainty in the frequency-comb measurement was well below the 1-kHz level within 100 s of measurement time (Table II), which is consistent with the frequency stability of LD2 described in Sec. II. However, we also observed a long-term frequency drift, which is described as "repeatability" in Table II, with typical values estimated to be 7.0kHz by using the frequency distribution of tens of experimental runs under the same conditions over 6 months by utilizing the $5P_{3/2}(F' = 3) - 4D_{5/2}(F'' = 3)$ transition of ^{87}Rb. Finally, we considered frequency pulling by adjacent spectral peaks. The approximated expression for the frequency shift by an adjacent Lorentzian peak is given in Appendix. The positions of the line center, full width at half maximum, and values at the maximum for each of the transitions were obtained via multi-Lorentzian curve fittings, which are indicated in Fig. 3 by red lines. The frequency shifts were calculated using Eq. (A8), and these are listed in Table II in parentheses. This shift becomes larger when the frequency spacing between two peaks reduces; the shift was largest for the $5P_{3/2}(F' = 4) - 4D_{5/2}(F'' = 5)$ transition of ^{85}Rb with a value of 15.8 kHz. In Table I, each of the absolute frequency values was corrected by these frequency shifts.

IV. HYPERFINE STRUCTURE CONSTANTS

The HFS constants can be calculated from the HFS splitting [6,8]. For the $5P_{3/2}(F' = 3) - 4D_{5/2}(F'' = 2, 3, 4)$ transitions of ^{87}Rb with the nuclear spin angular momentum $I = 3/2$, the HFS constants of $4D_{5/2}$ state of ^{87}Rb can be determined using the three absolute frequency values listed in Table I:

$$A^{87} = -\tfrac{4}{21} f^{87}(2'') + \tfrac{1}{12} f^{87}(3'') + \tfrac{3}{28} f^{87}(4''), \quad (1)$$

$$B^{87} = \tfrac{20}{21} f^{87}(2'') - \tfrac{5}{3} f^{87}(3'') + \tfrac{5}{7} f^{87}(4''), \quad (2)$$

where $f^{87}(F'')$ denotes the frequency of the $5P_{3/2}(F' = 3) - 4D_{5/2}(F'')$ transition of ^{87}Rb, A^{87} the magnetic dipole HFS constant, and B^{87} the electric quadrupole HFS constant. Similarly, the HFS constants of the $4D_{5/2}$ state of ^{85}Rb with nuclear spin angular momentum $I = 5/2$ is given as

$$A^{85} = -\tfrac{2}{9} f^{85}(3'') + \tfrac{1}{5} f^{85}(4'') + \tfrac{1}{45} f^{85}(5''), \quad (3)$$

$$B^{85} = \tfrac{50}{27} f^{85}(3'') - \tfrac{10}{3} f^{85}(4'') + \tfrac{40}{27} f^{85}(5''), \quad (4)$$

where $f^{85}(F'')$ denotes the frequency of the $5P_{3/2}(F' = 4) - 4D_{5/2}(F'')$ transition of ^{85}Rb, A^{85} the magnetic dipole HFS constant, and B^{85} the electric quadrupole HFS constant. The calculated HFS constants are summarized in Table III. The previously reported values are also listed in Table III, along with the corresponding references and experimental method used in each case. Figure 4 illustrates the comparison between these results.

The values of A^{87} and A^{85} agree well with the corresponding ones of Ref. [7] with uncertainties reduced by 2 orders

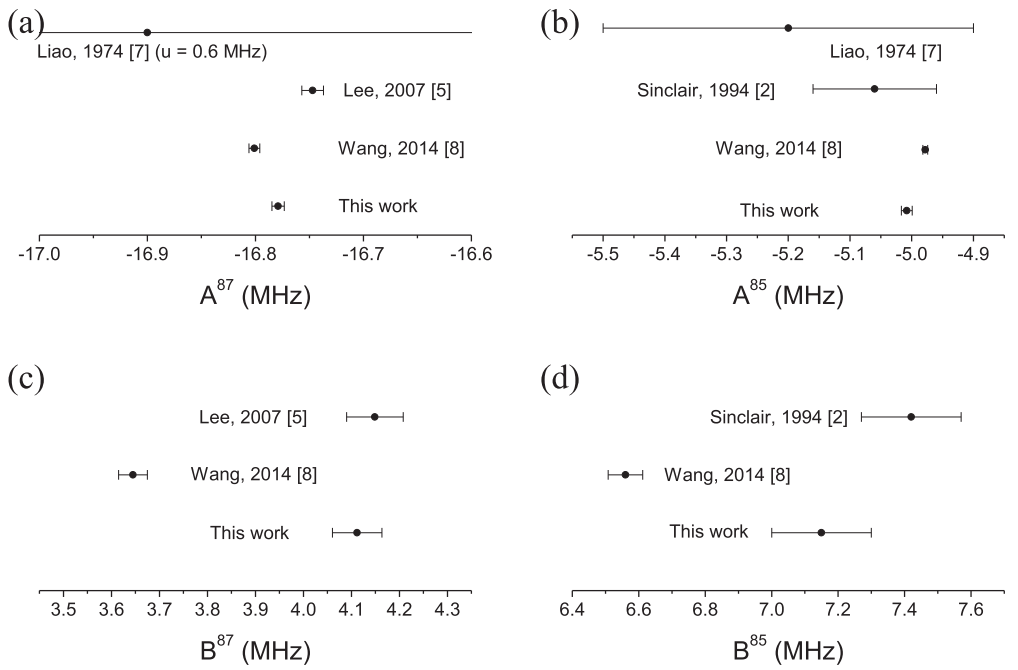

FIG. 4. Comparison between the measured values of hyperfine structure constants of $4D_{5/2}$ for and ^{85}Rb determined in this study and in previous ones. The corresponding references are indicated in square brackets. The measured hyperfine structure constants shown in the figure correspond to Fig. 4: (a) A^{87}, (b) A^{85}, (c) B^{87}, and (d) B^{85}. It is to be noted that the results of Ref. [5] (*) were obtained with linear-orthogonal polarization.

of magnitude. The values of A^{85} and B^{85} agree well with the corresponding ones in Ref. [2], and the uncertainty for the magnetic dipole HFS constant is decreased by an order of magnitude. As mentioned in the previous section, the results in Ref. [5] were obtained with linear-orthogonal polarization for LD1 and LD2, and thus this report provides the modified values for A^{87} and B^{87} with linear-parallel polarization. The HFS constants measured in this work do not agree with those in Ref. [8] within the uncertainties of each measurement. These discrepancies are larger with regard to the electric quadrupole constants, which is attributed to the fact that the electric quadrupole constant determination is more sensitive to the values of the frequency measurement of the HFS, as can be seen in Eqs. (1)–(4). One possible explanation for this difference is that the power level for LD2 was 3 times higher in Ref. [8] when compared with that in this study, which may have caused a change in the spectral profile in the DROP signal [4].

V. CONCLUSIONS

In conclusion, we measured the absolute frequency values of all (ten) of the excited-state hyperfine transitions of $5P_{3/2} - 4D_{3/2}$ and $5P_{3/2} - 4D_{5/2}$ for ^{85}Rb and ^{87}Rb atoms using a fiber femtosecond frequency-comb system, stabilizing a laser diode onto the line centers of the DROP spectra. The frequency uncertainties in measuring the absolute frequencies were rigorously evaluated by investigating the effects of the polarization angle, magnetic field, vapor cell dependence, laser power level, dc offset in the frequency lock, modulation depth of the laser frequency, short-term and long-term frequency stability, and frequency pulling by adjacent spectral peaks. This investigation yielded absolute frequency measurement values for two transitions, and furthermore, the uncertainty was reduced significantly for the other transitions. In addition, the absolute frequency measurement data were used to determine the HFS constants of $4D_{5/2}$ for ^{85}Rb and ^{87}Rb, and these were compared with previous reports. We believe that this report can aid in the comparison of various reports, since the complete data set of the transitions was obtained under the same conditions using the same method.

ACKNOWLEDGMENTS

This work was supported partly by the Korea Research Institute of Standards and Science under the project "Research on Time and Space Measurements," Grant No. 15011020, and also partly by the National Research Foundation of Korea (NRF), funded by the Ministry of Science, ICT, and future Planning (2015R1A2A1A05001819).

APPENDIX: FREQUENCY SHIFT BY AN ADJACENT LORENTZIAN PEAK

A Lorentzian function $L_1(x)$ is given by

$$L_1(x) = h_1 \frac{w_1^2}{4(x - x_{c1})^2 + w_1^2}, \tag{A1}$$

where x_{c1} is the center, w_1 is the full width at half maximum, and h_1 is the height (the value at the maximum). Its first and

second derivatives are given by

$$L_1'(x) = -8h_1w_1^2\frac{(x-x_{c1})}{\left[4(x-x_{c1})^2+w_1^2\right]^2}, \tag{A2}$$

$$L_1''(x) = \frac{8h_1w_1^2}{\left[4(x-x_{c1})^2+w_1^2\right]^3}\left[12(x-x_{c1})^2-w_1^2\right]. \tag{A3}$$

Next, we consider a function, which is the sum of two Lorentzian functions:

$$y(x) = L_1(x) + L_2(x). \tag{A4}$$

If $L_2(x)$ were not added, $y(x)$ would have the maximum at $x = x_{c1}$, with $L_1'(x_{c1}) = 0$. If we assume a small shift of α due to the presence of $L_2(x)$, it is expected by a Taylor expansion around $x = x_{c1}$,

$$y'(x_{c1}+\alpha) = y'(x_{c1}) + \alpha y''(x_{c1}) + O(\alpha^2) \sim y'(x_{c1}) + \alpha y''(x_{c1}) = 0. \tag{A5}$$

Using Eqs. (A2) and (A3),

$$y'(x_{c1}) = 8h_2w_2^2\frac{(x_{c2}-x_{c1})}{\left[4(x_{c2}-x_{c1})^2+w_2^2\right]^2}, \tag{A6}$$

$$y''(x_{c1}) = -\frac{8h_1}{w_1^2} + \frac{8h_2w_2^2}{\left[4(x_{c2}-x_{c1})^2+w_2^2\right]^3}\left[12(x_{c2}-x_{c1})^2-w_2^2\right]. \tag{A7}$$

Finally, the frequency shift by an adjacent Lorentzian peak can be approximated by

$$\alpha = -\frac{y'(x_{c1})}{y''(x_{c1})} = \frac{\left[4(x_{c2}-x_{c1})^2+w_2^2\right](x_{c2}-x_{c1})}{\frac{h_1}{h_2}\frac{1}{w_1^2w_2^2}\left[4(x_{c2}-x_{c1})^2+w_2^2\right]^3-\left[12(x_{c2}-x_{c1})^2-w_2^2\right]}. \tag{A8}$$

[1] H. Sasada, IEEE Photonics Technol. Lett. **4**, 1307 (1992).

[2] A. G. Sinclair, B. D. McDonald, E. Riis, and G. Duxbury, Opt. Commun. **106**, 207 (1994).

[3] H. S. Moon, W. -K. Lee, L. Lee, and J. B. Kim, Appl. Phys. Lett. **85**, 3965 (2004).

[4] H. S. Moon, L. Lee, and J. B. Kim, J. Opt. Soc. Am. B **24**, 2157 (2007).

[5] W. -K. Lee, H. S. Moon, and H. S. Suh, Opt. Lett. **32**, 2810 (2007); **40**, 2111(E) (2015).

[6] H. S. Moon, W.-K. Lee, and H. S. Suh, Phys. Rev. A **79**, 062503 (2009).

[7] K. H. Liao, L. K. Lam, R. Gupta, and W. Happer, Phys. Rev. Lett. **32**, 1340 (1974).

[8] J. Wang, H. Liu, G. Yang, B. Yang, and J. Wang, Phys. Rev. A **90**, 052505 (2014).

[9] M. S. Safronova and U. I. Safronova, Phys. Rev. A **83**, 052508 (2011).

[10] M. S. Safronova, W. R. Johnson, and A. Derevianko, Phys. Rev. A **60**, 4476 (1999).

[11] F. Adler, K. Moutzouris, A. Leitenstorfer, H. Schnatz, B. Lipphardt, G. Grosche, and F. Tauser, Opt. Express, **12**, 5872 (2004).

[12] J. Ye, S. Swartz, P. Jungner, and J. L. Hall, Opt. Lett. **21**, 1280 (1996).

[13] G. P. Barwood, P. Gill, and W. R. C. Rowley, Appl. Phys. B **53**, 142 (1991).

[14] A. Banerjee, D. Das, and V. Natarajanfz, Opt. Lett. **28**, 1579 (2003).